



Pharmaceutics, Drug Delivery and Pharmaceutical Technology

## Size and Charge Dependence of Ion Transport in Human Nail Plate



Sudhir M. Baswan, S. Kevin Li, Terri D. LaCount, Gerald B. Kasting\*

James L. Winkle College of Pharmacy, The University of Cincinnati Academic Health Center, Cincinnati, Ohio 45267-0004

## ARTICLE INFO

## Article history:

Received 11 September 2015  
 Revised 10 December 2015  
 Accepted 11 December 2015  
 Available online 23 January 2016

## Keywords:

diffusion  
 iontophoresis  
 membrane transport  
 mobility  
 nail  
 permeability  
 structure–transport relationship

## ABSTRACT

The electrical properties of human nail plate are poorly characterized yet are a key determinate of the potential to treat nail diseases, such as onychomycosis, using iontophoresis. To address this deficiency, molar conductivities of 17 electrolytes comprising 12 ionic species were determined in hydrated human nail plate *in vitro*. Cation transport numbers across the nail for 11 of these electrolytes were determined by the electromotive force method. Effective ionic mobilities and diffusivities at infinite dilution for all ionic species were determined by regression analysis. The ratios of diffusivities in nail to those in solution were found to correlate inversely with the hydrodynamic radii of the ions according to a power law relationship having an exponent of  $-1.75 \pm 0.27$ , a substantially steeper size dependence than observed for similar experiments in skin. Effective diffusivities of cations in nail were 3-fold higher than those of comparably sized anions. These results reflect the strong size and charge selectivity of the nail plate for ionic conduction and diffusion. The analysis implies that efficient transungual iontophoretic delivery of ionized drugs having radii upward of 5 Å (molecular weight, ca.  $\geq 340$  Da) will require chemical or mechanical alteration of the nail plate.

© 2016 American Pharmacists Association®. Published by Elsevier Inc. All rights reserved.

## Introduction

Onychomycosis accounts for nearly 50% of all nail disorders and affects 2%–18% or more of the world's population.<sup>1–6</sup> Although the condition is treatable, the current therapeutic options are limited due to efficacy and safety issues. Oral therapy for the treatment of onychomycosis is recommended by only 35%–65% of the physicians due to the associated side effects, such as headache, risk of hepatotoxicity, and potential drug–drug interactions.<sup>5</sup> The clinical significance of formulations, such as medicated nail lacquers, patches, and creams for topical treatment of onychomycosis, is debatable. New techniques, such as use of chemical penetration enhancers,<sup>7–10</sup> micro-drilling,<sup>11</sup> nail abrasion,<sup>12–14</sup> acid etching,<sup>15</sup> and iontophoresis,<sup>16–24</sup> are also being evaluated as potential treatment methods for onychomycosis. The drug–device combination that uses iontophoresis to deliver high concentrations of medication directly to the site of action has considerable potential to improve the treatment of onychomycosis.<sup>16–24</sup> Although significant efforts have been made to evaluate and enhance transungual iontophoretic

drug delivery, little has been performed to systematically characterize ion transport across the nail plate. It is fair to say that work to date on transungual ion transport has been largely phenomenological, with little guidance from electrotransport theory.

The main objective of this research was to evaluate the impact of ionic size and charge on transungual transport of both organic and inorganic ions. Transport parameters including ionic conductance at infinite dilution, ionic mobility, and diffusion coefficient of 12 ionic species in hydrated nail plate were obtained by performing conductivity and transport number studies using *in vitro* electrochemical and radiochemical methods. Also, gravimetric experiments were performed to determine the extent of hydration and keratin fiber volume fraction of the nail plate. Results are compared with similar information obtained recently for charged solutes in human stratum corneum<sup>25</sup> as amended<sup>26</sup> and to passive diffusion data for uncharged solutes in human nail plate.<sup>27</sup> A procedure for using the conductivity results to predict transungual iontophoretic drug delivery is proposed.

## Materials and Methods

## Materials

Sodium chloride (NaCl), potassium chloride (KCl), calcium chloride (CaCl<sub>2</sub>), and potassium bromide (KBr) were obtained from

This article contains supplementary material available from the authors upon request or via the Internet at <http://dx.doi.org/10.1016/j.xphs.2015.12.011>.

\* Correspondence to: Gerald B. Kasting (Telephone: +1-513-558-1817; Fax: +1-513-558-0978).

E-mail address: [gerald.kasting@uc.edu](mailto:gerald.kasting@uc.edu) (G.B. Kasting).

<http://dx.doi.org/10.1016/j.xphs.2015.12.011>

0022-3549/© 2016 American Pharmacists Association®. Published by Elsevier Inc. All rights reserved.

Fisher Scientific (Pittsburgh, PA); sodium bromide (NaBr), sodium sulfate (Na<sub>2</sub>SO<sub>4</sub>), tetraethylammonium bromide (TEABr), tetraethylammonium chloride (TEACl), sodium acetate (Na-Ac), tetraethylammonium acetate (TEA-Ac), tetraphenylphosphonium bromide (TPPBr), tetraethylammonium benzoate (TEA-Bz), and olamine hydrochloride (Olam-Cl) from Sigma-Aldrich (St. Louis, MO); calcium bromide (CaBr<sub>2</sub>) and potassium sulfate (K<sub>2</sub>SO<sub>4</sub>) from GFS Chemicals (Powell, OH); sodium benzoate (Na-Bz) from Alfa Aesar (Ward Hill, MA); and methyltriphenylphosphonium bromide (MTPPBr) from Strem Chemicals (Newburyport, MA). CaCl<sub>2</sub> and CaBr<sub>2</sub> had stated purity of ≥96%, TPPBr ≥97%, MTPPBr ≥98%, and the rest of the chemicals were ≥99% pure. KCl conductivity standard solutions (1000 and 10,000 μmho/cm at 25°C) were obtained from LabChem Inc. (Pittsburgh, PA). All aqueous solutions were prepared in deionized (DI) water (18.2 MΩ cm at 25°C, US Filter). Dialysis membranes (MWCO 6000 Da) were obtained from Bel-Art Products (Wayne, NJ). Optically clear silicone elastomer MED-6033 was obtained from NuSil Technology LLC (Carpinteria, CA). <sup>22</sup>NaCl (100–2000 Ci/g) and <sup>14</sup>C-TEABr (3.5 mCi/mmol) were purchased from PerkinElmer Life and Analytical Sciences (Boston, MA). Ag-AgCl electrodes, E215, and E252P were obtained from In-Vivo Metric (Healdsburg, CA).

#### Nail Sample Preparation

Frozen, human cadaver fingernails (Caucasian men, age 26–86) were obtained from Science Care Anatomical (Phoenix, AZ). A total of 75 index, middle, and ring fingernails from both left and right hands of 13 donors were selected for the experiments. The frozen nail plates were thawed at room temperature (25 ± 2°C) in DI water and cleaned by removing adhering tissues with forceps and cotton swabs. The nails were then rinsed with DI water and inspected for any visual deformities, such as cracks or hairline fractures. The thickness of nail plates, ranging from 0.21 to 0.85 mm, was measured using a point micrometer (Mitutoyo, Kawasaki, Kanagawa, Japan). The use of human cadaver nails was approved by the Institutional Review Board at the University of Cincinnati (Cincinnati, OH).

#### Nail Adapter Preparation

The nail adapters were fabricated from a thermally curable silicone elastomer MED-6033, which comprised 2 parts. These materials were mixed together in equal proportions by volume and allowed to stand for 2–3 h to remove air bubbles formed during the mixing process, before pouring into the molds. The silicone mix within the molds was then cured for 30 minutes at 60 ± 2°C to form sturdy but flexible nail adapter halves. A circular hole, 9 mm in diameter (0.64 cm<sup>2</sup>), was punched in the center of both halves of the silicone nail adapter. The shape and design of these custom-made silicone nail adapters were similar to Teflon nail adapters made by PermeGear Inc. (Bethlehem, PA); however, they had an additional advantage of not requiring adhesive glue, which is used to seal the gaps between the nail and Teflon nail adapters. These custom-made silicone nail adapters accommodated the nail curvature better than Teflon adapters and demonstrated no inter-compartmental leakage in preliminary experiments.

#### Nail Hydration Studies

Hydration experiments were performed on 6 fingernails selected randomly from different donor sets. Nail plates were immersed in DI water in a glass vial and placed in a water bath (32.0 ± 0.1°C) for 24 h. The nail samples were removed after 24 h, excess water was wiped off with Kimwipes® and cotton swabs, and

then wet mass ( $m_{\text{wet}}$ ) of the nail plate was measured on an analytical balance (Mettler Toledo AB-135SP®) reading to ±0.01 mg. The nail samples were then dried at 60°C overnight or until constant weight was achieved ( $m_{\text{dry}}$ ). The water content  $w$  (wt%) in hydrated nail plate was determined by Equation 1. The water uptake capacity of dry nail plate ( $v'$ ) was determined using Equation 2.

$$w(\text{wt } \%) = \frac{m_{\text{wet}} - m_{\text{dry}}}{m_{\text{wet}}} \times 100\% \quad (1)$$

$$v'(\text{g H}_2\text{O/g dry nail}) = \frac{m_{\text{wet}} - m_{\text{dry}}}{m_{\text{dry}}} \quad (2)$$

Assuming nail plate to comprise only keratin and water, the fiber volume fraction ( $\phi_f$ ) is given by<sup>28</sup>:

$$\phi_f = 1 - \frac{\rho_m v'}{\rho_1 + \rho_m v'} \quad (3)$$

where  $\rho_m$  is the density of dry nail (keratin density ~1.3 g/cm<sup>3</sup>)<sup>29</sup> and  $\rho_1$  is the density of water (~1.0 g/cm<sup>3</sup>).

#### Conductivity Measurements

The molar conductivities of all the electrolyte solutions and of human nail plate immersed there were determined by a 4-terminal resistance method<sup>25,30,31</sup> in side-by-side diffusion cells (PermeGear Inc.). The method was that used in Franz diffusion cells by LaCount and Kasting<sup>25</sup> except for variations as described subsequently. Commercially available cylindrical Ag-AgCl electrodes, E215 and E252P (In-Vivo Metric), were used for all electrolytes except for those containing bromide. For the latter, homemade Ag-AgBr electrodes were used as Ag-AgCl electrodes are fouled by bromide ions.<sup>32</sup> Ag-AgBr electrodes were constructed from a 1.0-mm diameter silver wire (99.999%; Alfa Aesar) electrolyzed in 0.1 M KBr solution and were stored in the dark before use due to its sensitivity to light. Electrodes were placed as shown in Figure 1. The 98.28 kΩ standard resistor described previously<sup>25</sup> was replaced by a 10.01 kΩ (±0.02%) precision standard resistor (Ohm-labs Inc., Pittsburgh, PA) to better match the 3–10 kΩ resistance of the hydrated nail plate immersed in physiological saline solution.<sup>33</sup> A 10 V peak-to-peak, 20 Hz sinusoidal signal was applied across a 1 MΩ current-limiting resistor using a waveform generator (Agilent 33220A) to yield a 6.5–6.9 μA root mean square AC current across the nail plate. The AC potential generated across the nail plate (maximum of 0.5 V peak to peak) was measured by the inner pair of electrodes using a sensitive multimeter (Agilent 34410A).

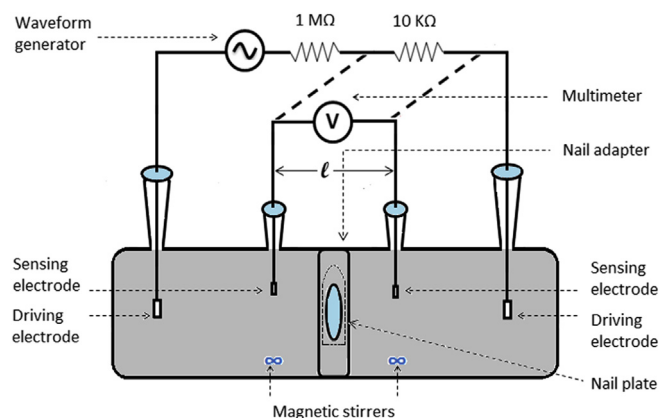


Figure 1. Diffusion cell configuration for 4-terminal resistance measurements.

The multimeter was alternatively connected to the 10 k $\Omega$  standard resistor by a double-pole double-throw toggle switch (represented by broken lines in Fig. 1) that facilitated the measurement of potential drop across the standard. The use of low-magnitude, low-frequency AC signals ensures that the treatment has little impact on tissue electrical properties and that the impedance is primarily resistive rather than capacitive in nature.<sup>34</sup>

Solution-only measurements were made at 25°C with the nail adapter in place but without the nail plate. Cell constants  $K$  (per centimeter), corresponding to the effective ratio of path length  $l$  to cross-sectional area  $A$ , were determined by a 2-point calibration using KCl standards (1000 and 10,000  $\mu\text{mho/cm}$  at 25°C). The average distance  $l$  between the sensing electrodes was 2.7 cm and varied from one cell to another by  $\pm 0.3$  cm due to inherent variation in cell design. The resistance imparted by each electrolyte,  $R_{\text{soln}}$  ( $\Omega$ ), was measured at 8 concentrations in the range 0.007–0.154 M for monovalent electrolytes and 0.007–0.077 M for polyvalent electrolytes. These values were converted to molar conductivity of the electrolytes  $\Lambda_{\text{soln}}$  ( $\text{cm}^2/\text{mol } \Omega$ ) using the relationship  $\Lambda_{\text{soln}} = K/(R_{\text{soln}}c)$ , where  $c$  is the electrolyte concentration expressed in moles per cubic centimeter. Molar conductivity at infinite dilution,  $\Lambda_{\text{soln}}^0$ , was calculated as the y-intercept of a plot of  $\Lambda_{\text{soln}}$  versus  $\sqrt{c}$ , that is, the Kohlrausch plot.<sup>25</sup> Values of  $\Lambda_{\text{soln}}^0$  so determined were compared with literature values<sup>35</sup> to test the accuracy of the method.

For the nail conductivity measurements, cadaveric human nail plates (3 per electrolyte) were placed between the nail adapters within the diffusion cells, and the temperature was maintained at  $32.0 \pm 0.1^\circ\text{C}$ . The samples were hydrated for 24 h in DI water and then exposed to increasing concentrations of electrolytes in the same range as the solution experiments. Each concentration was maintained for a duration of 24 h before measuring the resistance, yielding a total study time of 9 days for each nail sample. The electrolyte solutions were used without pH adjustment to avoid any contribution to conductivity from buffering ions. The pH values of all the solutions were measured to be in the range 5.5–7.5 before the experiment and 5.6–7.8 after the experiment.

The resistance measured in this leg of the study,  $R_{\text{total}}$ , contains contributions from both the nail and solution, that is,  $R_{\text{total}} = R_{\text{nail}} + R_{\text{soln}}$ . To obtain  $R_{\text{nail}}$ ,  $R_{\text{soln}}$  values at 25°C at each concentration (obtained from the solution-only experiments) were first corrected to 32°C by multiplying by the water viscosity ratio,  $\eta^{32}/\eta^{25} = 0.765\text{cp}/0.891\text{cp} = 0.859$ , and then subtracted from  $R_{\text{total}}$ . Values of  $R_{\text{nail}}$  so calculated were found to comprise 85% to 98% of  $R_{\text{total}}$ . Nail-specific resistivity values,  $\rho_{\text{nail}} = R_{\text{nail}}A/L$ , were calculated using the exposed cross-sectional area ( $A$ ) and thickness ( $L$ ) of the nail sample and then converted to effective molar conductivities in nail ( $\text{cm}^2/\text{mol } \Omega$ ) using the relationship  $\Lambda_{\text{nail}} = 1/(\rho_{\text{nail}}c)$ , where  $c$  is the “external” electrolyte concentration expressed in moles per cubic centimeter. Note that this calculation does not use the cell constant  $K$ . There is an assumption built into the calculation that will be discussed later, namely the use of the external electrolyte concentration to calculate  $\Lambda_{\text{nail}}$ .

The limiting molar conductivity at infinite dilution ( $\Lambda_{\text{nail}}^0$ ) was determined from the Kohlrausch plot. For all the nail experiments, the 2 lowest concentration data were excluded from the fit because significant positive deviations from the Kohlrausch law were observed. Conductivity data for selected electrolytes in solution and nail plate are included in the [Supplementary Material](#).

#### Transport Number Measurements

The stationary state electromotive force (EMF) method<sup>25,36–41</sup> was used to determine cation transport numbers for the

electrolytes yielding reversible electrode reactions, namely chloride- and bromide-containing electrolytes, and for nail plates immersed there. Ag–AgCl electrodes were used for the  $\text{Cl}^-$  electrolytes and Ag–AgBr electrodes for  $\text{Br}^-$  electrolytes. Thus, a total of 22 cation transport numbers were determined, 11 in solution and 11 in nail. Solution transport number measurements were conducted at 25°C using 2 dialysis membranes to separate the 2 compartments as described by LaCount and Kasting.<sup>25</sup> The peak EMF values were measured after 30–45 s.

The nail transport number experiments were performed at 32°C on the same samples used in conductivity experiments to reduce variability. After the conductivity experiments, the nails were equilibrated for 24 h with electrolyte solution at the highest concentration under consideration (0.154 M for monovalent electrolytes and 0.077 M for polyvalent electrolytes). The solution in the left compartment (facing the dorsal side of nail) was then replaced with fresh solution of the same concentration ( $c_1$ ), and the solution in the right compartment was varied from 0.0125 to 0.077 M ( $c_2$ ) ensuring that the concentration ratio  $c_1/c_2$  was always  $\geq 2$ . Five different concentration ratios were evaluated: 12.3, 7.7, 4.4, 3.1, and 2. At each concentration ratio, the system was allowed to equilibrate for 4 h. The solutions in both the chambers were then replaced with fresh solutions of the same concentrations, and the stationary state EMF (volts) was measured after an additional 4 h by inserting 2 pre-equilibrated electrodes connected to the Agilent 34410A multimeter. The system was magnetically stirred to minimize boundary layer effects on the measured potential.<sup>36</sup> The dimensionless mean cation transport number ( $t_{m+}$ ) was calculated as<sup>36–39</sup>:

$$\text{EMF} = \frac{v}{v_+} \frac{RT}{F} \frac{t_{m+}}{z_+} \ln \frac{c_2 \gamma_{2\pm}}{c_1 \gamma_{1\pm}} \quad (4)$$

where  $v = \sum v_{\pm}$  is the total number of cations and anions per mole of salt,  $R$  is the gas constant (8.314 J/K/mol),  $T$  is temperature (K),  $F$  is Faraday's constant (96,485 C/mol),  $z_+$  is the cation valence, and the  $\gamma_{i\pm}$  are mean ionic activity coefficients calculated according to the extended Debye–Huckel theory.<sup>42</sup>

$$\log \gamma_{\pm} = \frac{Bz_1z_2\sqrt{\mu}}{1 + \sqrt{\mu}} \quad (5)$$

In Equation 5,  $B$  is a constant having a value 0.509 for water at 25°C and 0.516 at 32°C and  $\mu$  is the ionic strength.

For radiochemical transport measurements, nail samples were prepared, mounted, and hydrated in side-by-side diffusion cells as described earlier. Cation transport numbers of NaCl and TEACl were determined under symmetrical, fully hydrated conditions at 3 different concentrations (0.007, 0.04, and 0.154 M). The donor and receptor chambers were filled with unlabeled solutions of NaCl (or TEACl) of same molarity and allowed to equilibrate for 24 h. After 24 h, the donor and receptor chambers were replaced with fresh unlabeled solutions. The donor chamber was then spiked with 1  $\mu\text{Ci}$   $^{22}\text{NaCl}$  (100–2000 Ci/g) or  $^{14}\text{C}$ -TEABr (3.5 mCi/mmol). Ag–AgCl electrodes prepared by electrolyzing Ag strip (99.9% purity; Alfa Aesar) in 0.1 N KCl solution were placed in the receptor compartment and Ag electrodes in the donor compartment. A constant direct current iontophoretic device, Phoresor II Auto, model PM 850 (Iomed, Inc., Salt Lake City, UT), was used to drive the system, with the Ag electrode serving as the anode. A custom-made variable potentiometer was used to reduce the 100  $\mu\text{A}$  minimum current supplied by the device to 10  $\mu\text{A}$ . The resistance of the nail plate plus intervening solution was measured by the 4-terminal technique before the experiment and periodically thereafter. This was useful

in adjusting the potentiometer to yield the desired current. The test durations for  $^{22}\text{Na}^+$  and  $^{14}\text{C-TEA}^+$  experiments were 16 and 56 h, respectively.

Aliquots of the donor solution (10  $\mu\text{L}$ ) and receptor solution (2 mL) were removed at predetermined time intervals. The receptor solution was replaced with 2 mL of fresh unlabeled electrolyte solution to maintain a constant volume. The samples were mixed with 10 mL of UltimaGold™ scintillation fluid (PerkinElmer Life and Analytical Sciences, Shelton, CT) and analyzed with a liquid scintillation counter (LS6500; Beckman Counter Inc., Fullerton, CA). The steady-state flux of the permeant  $J_i$  (mol/cm<sup>2</sup>/s) across the nail plate was calculated from the slope of the linear portion of the plot of cumulative moles of permeant transported across the nail plate per unit area versus time. The transport number for the radiolabeled species was calculated from the steady-state flux and the current density  $I$  (A/cm<sup>2</sup>) as:

$$t_i = \frac{|z_i|FJ_i}{I} \quad (6)$$

### Data Analysis

Data were analyzed as described in LaCount and Kasting<sup>25</sup> but with the corrected membrane thickness given later.<sup>26</sup> According to Kohlrausch's law of independent migration of ions, the term  $\Lambda^0$  can be decomposed into additive contributions from the individual ionic species and is given as<sup>35,43</sup>:

$$\Lambda^0 = \sum v_i \lambda_i \quad (7)$$

Here,  $v_i$  is the number of equivalents of species "i" per mole of salt and  $\lambda_i$  is its limiting equivalent conductance at infinite dilution. The relationship between transport number  $t_i^0$  and molar conductivity at infinite dilution is given as<sup>35</sup>:

$$t_i^0 = v_i \lambda_i / \Lambda^0 \quad (8)$$

A nonlinear minimization procedure was performed on the 17 conductivity relationships (Eq. 7) and 11 transport number relationships (Eq. 8) for both nail and solution data to yield optimized values of  $\lambda_i$  for the 12 ionic species in the study.<sup>25</sup> The conventional ionic mobilities ( $u_i^0$ ) in square centimeter per volt second and ionic diffusivities ( $D^0$ ) in square centimeter per second at infinite dilution were calculated using the relationships  $u_i^0 = \lambda_i / |z_i|F$  and  $D^0 = u_i^0 RT / |z_i|F$ , respectively.<sup>35</sup> Because nail plate is not a homogeneous medium, we will refer to mobility and diffusivity values so obtained in this medium as "effective" values.

Hydrodynamic radii were calculated according to the Stokes–Einstein relationship,<sup>35</sup>

$$r_{SE} = k_b T / 6 \pi \eta D^0 \quad (9)$$

Here  $k_b$  is Boltzmann's constant ( $1.3806 \times 10^{-16}$  erg/K),  $T$  is absolute temperature (K), and  $\eta$  is the viscosity of water (0.00891 poise at 25°C). As a comparative measure of size, hydrated ionic radii ( $r_H$ ) were obtained from the literature using the values proposed by Nightingale.<sup>44</sup> Values which were not published were read from the calibration curve<sup>44</sup> using WebPlotDigitizer, version 2.5. These values are larger than  $r_{SE}$  for solutes for which  $r_{SE} < 5 \times 10^{-8}$  cm (5 Å). A third measure of size, originally proposed by Gierer and Wirtz<sup>45</sup> for small, uncharged solutes, was also considered. The rationale for focusing the analysis on  $r_{SE}$  is discussed in the [Supplementary Material](#).

## Results

### Nail Hydration Studies

The water content of the fully hydrated nail plate was found to be  $w = 31 \pm 2\%$  (mean  $\pm$  SD,  $n = 6$ ). This value falls within the range of values reported in the literature (28%–34%).<sup>7,8,28,46</sup> The water uptake capacity of dry nail was found to be  $v' = 0.44 \pm 0.05$  g H<sub>2</sub>O/g dry nail. The keratin fiber volume fraction was calculated to be  $\phi_f = 0.64 \pm 0.02$ .

### Conductivity Measurements

Equivalent conductances at infinite dilution of 17 electrolytes in solution ( $\Lambda_{\text{soln}}^0$ ) and nail plate ( $\Lambda_{\text{nail}}^0$ ) are listed in [Table 1](#). Conductance values in the nail plate were reduced relative to those in free solution by factors ranging from 440 to 1380.

### Transport Experiments

Cation transport numbers of 11 electrolytes in solution ( $t_{+\text{soln}}^0$ ) and hydrated nail plate ( $t_{+\text{nail}}^0$ ) determined by the EMF method are listed in [Table 2](#). Transport numbers calculated from the regressed values of the individual ionic conductances and electrolyte composition are also presented. The ratio  $t_{+\text{nail}}^0 / t_{+\text{soln}}^0$  is shown in the last column. This ratio was significantly  $>1$  for the small, monovalent ions  $\text{Na}^+$  and  $\text{K}^+$ , close to 1 for the medium-sized tetramethyl ammonium ( $\text{TEA}^+$ ) and olamine ( $\text{OlamH}^+$ ) ions, and significantly  $<1$  for  $\text{Ca}^{2+}$  and the large, monovalent ions methyl triphenylphosphonium ( $\text{MTPP}^+$ ) and tetraphenylphosphonium ( $\text{TPP}^+$ ).

The transport numbers of  $\text{Na}^+$  and  $\text{TEA}^+$  ions in nail plate immersed in their respective chloride solutions determined by the radiochemical method are shown in [Figure 2](#). Two-way ANOVA ( $\alpha = 0.05$ ), blocking on treatment and nail sample, showed that there were no significant differences between values determined by radiochemical and EMF methods. The lag times for achieving steady-state flux for  $^{22}\text{Na}^+$  and  $^{14}\text{C-TEA}^+$  experiments were approximately 4 and 20 h, respectively. Electrical current was

**Table 1**  
Limiting Equivalent Conductance Values (Mean  $\pm$  SD) of Electrolytes in Aqueous Solution ( $\Lambda_{\text{soln}}^0$ ) and Hydrated Nail Plate ( $\Lambda_{\text{nail}}^0$ ) at Infinite Dilution

Electrolyte	$\Lambda_{\text{soln}}^0$ <sup>a</sup> (cm <sup>2</sup> /mol $\Omega$ )		$\Lambda_{\text{nail}}^0$ <sup>b</sup> (cm <sup>2</sup> /mol $\Omega$ )	$\Lambda_{\text{nail}}^0 / \Lambda_{\text{soln}}^0$ <sup>c</sup> $\times 100$
	Observed	Literature <sup>d</sup>		
NaCl	126.4 $\pm$ 1.7	126.4	0.277 $\pm$ 0.030	0.188
NaBr	127.3 $\pm$ 1.7	128.2	0.293 $\pm$ 0.031	0.196
Na-Ac	89.2 $\pm$ 1.0	91.0	0.208 $\pm$ 0.027	0.196
Na-Bz	82.6 $\pm$ 1.8	82.4	0.212 $\pm$ 0.004	0.221
KCl	149.2 $\pm$ 3.4	149.8	0.372 $\pm$ 0.026	0.213
KBr	150.7 $\pm$ 3.2	151.6	0.399 $\pm$ 0.025	0.226
TEACl	108.8 $\pm$ 1.7	108.9	0.161 $\pm$ 0.016	0.127
TEABr	113.9 $\pm$ 1.7	110.7	0.174 $\pm$ 0.023	0.135
TEA-Ac	72.6 $\pm$ 0.7	73.5	0.061 $\pm$ 0.011	0.071
TEA-Bz	64.8 $\pm$ 2.0	64.9	0.065 $\pm$ 0.005	0.086
MTPPBr	100.2 $\pm$ 0.6	—	0.163 $\pm$ 0.011	0.140
TPPBr	93.4 $\pm$ 0.9	—	0.158 $\pm$ 0.005	0.145
Olam-HCl	116.9 $\pm$ 1.2	118.5	0.190 $\pm$ 0.012	0.138
½ CaCl <sub>2</sub>	135.9 $\pm$ 9.9	135.8	0.191 $\pm$ 0.032	0.121
½ CaBr <sub>2</sub>	135.9 $\pm$ 10.3	137.6	0.235 $\pm$ 0.024	0.147
½ Na <sub>2</sub> SO <sub>4</sub>	130.7 $\pm$ 5.9	130.1	0.201 $\pm$ 0.019	0.133
½ K <sub>2</sub> SO <sub>4</sub>	149.3 $\pm$ 4.5	153.5	0.260 $\pm$ 0.027	0.145

<sup>a</sup> 25°C.

<sup>b</sup> 32°C.

<sup>c</sup>  $\Lambda_{\text{soln}}^0$  experimental values corrected to 32°C by multiplying by the viscosity ratio,  $\eta^{25}/\eta^{32} = 1.165$ .

<sup>d</sup> Robinson and Stokes.<sup>35</sup>

**Table 2**  
Cation Transport Numbers  $t_+^0$  in Solution and Nail Plate

Electrolytes	Solution			Nail		$t_{+,\text{nail}}^0/t_{+,\text{soln}}^0$ <sup>f</sup>
	Obs <sup>a</sup>	Calc <sup>b</sup>	Lit <sup>c</sup>	Obs <sup>d</sup>	Calc <sup>e</sup>	
NaCl	0.392 ± 0.005	0.390	0.40	0.581 ± 0.012	0.577	1.48
NaBr	0.385 ± 0.003	0.386	0.39	0.552 ± 0.005	0.545	1.41
KCl	0.495 ± 0.005	0.486	0.49	0.685 ± 0.007	0.655	1.35
KBr	0.484 ± 0.006	0.482	0.48	0.622 ± 0.015	0.625	1.30
TEACl	0.280 ± 0.005	0.279	0.30	0.297 ± 0.006	0.314	1.13
TEABr	0.273 ± 0.008	0.275	0.29	0.321 ± 0.029	0.287	1.04
Olam-HCl	0.356 ± 0.0003	0.354	0.36	0.362 ± 0.016	0.359	1.01
CaCl <sub>2</sub>	0.381 ± 0.027	0.392	0.44	0.186 ± 0.018	0.222	0.57
CaBr <sub>2</sub>	0.389 ± 0.004	0.388	0.43	0.206 ± 0.003	0.201	0.52
MTPPBr	0.194 ± 0.006	0.194	–	0.045 ± 0.003	0.045	0.23
TPPBr	0.183 ± 0.009	0.182	–	0.050 ± 0.013	0.050	0.27

<sup>a</sup> Experimental value (mean ± SD) by EMF method at 25°C.

<sup>b</sup> Calculated from Equation 8 using the values of  $\lambda_i$  in column 3 of Table 3.

<sup>c</sup> Calculated from Equation 8 using the values of  $\lambda_i$  in column 4 of Table 3.

<sup>d</sup> Experimental value (mean ± SD) by EMF method at 32°C.

<sup>e</sup> Calculated from Equation 8 using the values of  $\lambda_i$  in column 2 of Table 3.

<sup>f</sup> Ratio of columns 6–3.

nearly constant throughout the experiments, although a slight variation (~5%–14% increase) was observed in a few samples for <sup>14</sup>C-TEA<sup>+</sup>. This fluctuation may be attributed to variation in nail plate resistance (tissue condition) over the 56-h test period. Average current over the test period was used to calculate transport numbers. The variability associated with the change in current over time for <sup>14</sup>C-TEA<sup>+</sup> was less than the inter-nail variability.

#### Effective Ionic Mobilities and Diffusivities in Nail Plate

Calculated values of individual ionic conductivities, mobilities, and diffusivities at infinite dilution of the 12 ionic species in

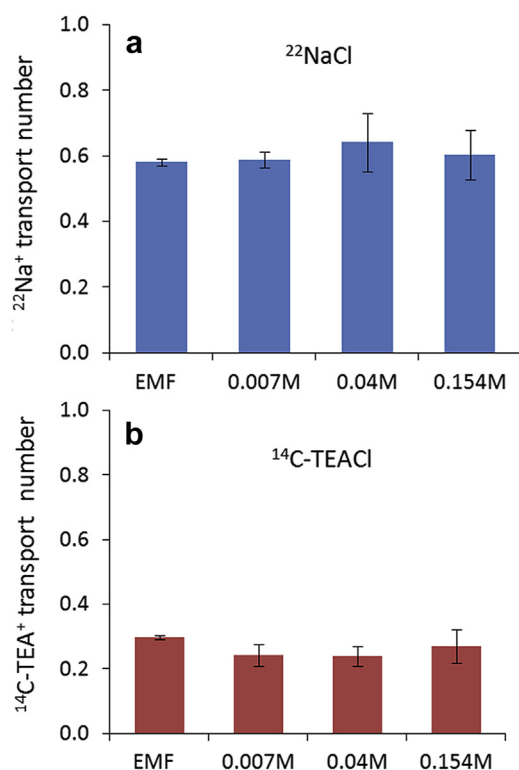


**Figure 2.** Cation transport numbers in hydrated nail plate for (a) NaCl and (b) TEACl determined by the radiochemical method. The first column in each panel shows the mean value determined by the EMF method (column 5 of Table 2).

hydrated nail plate are listed in Table 3. The aqueous diffusivities of these ions and 2 measures of their size are listed in Table 4.

To isolate the effects of the nail plate from the known behavior of ions in solution, we prepared log–log plots of the ratio of effective ionic diffusivity in nail ( $D_{\text{nail}}^0$ ) to that in solution ( $D_{\text{soln}}^0$ ) versus the hydrodynamic radius of each ion,  $r_{\text{SE}}$ . This ratio directly shows the impact of diffusive hindrance in the nail, above and beyond the resistance of the aqueous medium. The results are shown in Figure 3. It is evident that values of  $D_{\text{nail}}^0/D_{\text{soln}}^0$  for cations at any given radius are higher than those for anions. Values are inversely related to ionic radius, with more scatter evident among the anions. It should be noted that  $D_{\text{nail}}^0$  values for sulfate, benzoate, and acetate ions were imprecisely determined (cf. the  $\lambda_i$  values in Table 3) due to the small number of electrolytes and lack of transport number measurements for these species. The value for sulfate was particularly low. On account of this and the fact that its behavior in aqueous solution is already unusual,<sup>42</sup> sulfate ion was excluded from the remainder of the analysis. Although this decision may be arbitrary, inclusion of sulfate would not qualitatively change the results that follow.

Linear regression of the data in Figure 3 was conducted under the hypothesis that the magnitude of the effective ionic diffusivities in nail could be different for cations and anions, but the size dependence should be the same. Thus, the slopes of the lines for cations were constrained to the same values. The regression equations were then transformed to power laws by taking the antilog. This procedure yielded

$$\begin{aligned} D_{\text{nail}}^0/D_{\text{soln}}^0 = & 0.00522r_{\text{SE}}^{-1.75} \text{ cations} \\ & 0.00170r_{\text{SE}}^{-1.75} \text{ anions} \end{aligned} \quad (10)$$

$$n = 11; s = 0.168; r^2 = 0.851$$

where the root mean square deviation  $s$  is expressed in base-10 log units. Equation 10 shows that the effective diffusivity of cations in nail plate exceeds that of comparably sized anions by a factor of  $522/170 = 3.07$ . We argue below that this difference actually reflects more favorable partitioning of cations than anions into the negatively charged nail plate, as would be expected from a Donnan equilibrium,<sup>47</sup> rather than higher intrinsic mobility.

Unconstrained fits of the data in Figure 3 in which the slopes of the regression lines for cations and anions were allowed to differ gave nearly the same results as Equation 10, when sulfate ion was excluded from the analysis. This was not the case when the hydrated radius,  $r_{\text{H}}$ , was substituted for the hydrodynamic radius,  $r_{\text{SE}}$ . The use of  $r_{\text{H}}$  also gave much steeper slopes because the hydrated radii for very small ions greatly exceed their hydrodynamic radii (cf. Table 4, columns 5 and 6).

#### Discussion

Passive diffusion studies of uncharged solutes permeating human nail plate have shown little dependence on lipophilicity but a steep dependence on size.<sup>48</sup> This result led these investigators and others<sup>49,50</sup> to describe nail as a “hydrophilic gel membrane,” with resistance to diffusion provided by the keratin fibers suspended in a continuous aqueous medium. Notably, both Kobayashi et al.<sup>48</sup> and Mertin and Lippold<sup>49</sup> found that nail was less permeable to ionic solutes than to uncharged solutes, in contrast to earlier findings by Walters et al.<sup>51</sup> They discussed this finding in the context of Donnan exclusion of charged compounds from the negatively charged nail plate. Yet, the electrostatic coupling between cationic and anionic species in these passive diffusion experiments complicates this picture. The 2 species must diffuse together.<sup>52</sup>

**Table 3**  
Limiting Ionic Conductances ( $\lambda_i$ ), Effective Mobilities ( $u^0$ ), and Effective Diffusivities ( $D^0$ ) calculated from the data in Tables 1 and 2

Ionic species	$\lambda_i$ (cm <sup>2</sup> /mol $\Omega$ )			$u^0 \times 10^5$ (cm <sup>2</sup> /V s)		$D^0 \times 10^7$ (cm <sup>2</sup> /s)	
	Nail <sup>a,b</sup>	Soln <sup>c</sup>	Literature <sup>d</sup>	Nail <sup>a</sup>	Nail <sup>a</sup>	Nail <sup>a</sup>	Nail <sup>a</sup>
Na <sup>+</sup>	0.182 ± 0.023	51.0 ± 4.9	50.1	0.188		0.495	
K <sup>+</sup>	0.253 ± 0.030	75.3 ± 6.5	73.5	0.262		0.688	
TEA <sup>+</sup>	0.061 ± 0.011	30.7 ± 3.5	32.6	0.063		0.166	
Ca <sup>2+</sup>	0.076 ± 0.017	102.8 ± 8.6	119.0	0.039		0.052	
OlamH <sup>+</sup>	0.075 ± 0.018	43.6 ± 6.3	42.2	0.077		0.203	
TPP <sup>+</sup>	0.008 ± 0.009	18.0 ± 3.9	—	0.008		0.022	
MTPP <sup>+</sup>	0.007 ± 0.009	19.5 ± 3.9	—	0.007		0.020	
Cl <sup>-</sup>	0.133 ± 0.014	79.6 ± 5.2	76.3	0.138		0.362	
Br <sup>-</sup>	0.151 ± 0.016	80.9 ± 5.2	78.1	0.157		0.412	
SO <sub>4</sub> <sup>2-</sup>	0.027 ± 0.064	153.7 ± 20.0	160.0	0.014		0.018	
Bz <sup>-</sup>	0.017 ± 0.051	32.9 ± 18.2	32.3	0.018		0.047	
Ac <sup>-</sup>	0.013 ± 0.051	40.1 ± 18.2	40.9	0.014		0.036	

<sup>a</sup> 32°C.

<sup>b</sup> Values given as mean ± 67% confidence limit.

<sup>c</sup> 25°C; values given as mean ± 95% confidence limit.

<sup>d</sup> Literature values in solution at 25°C.<sup>35</sup>

Conductivity measurements yield a different limit in which electrostatically coupled diffusion is overwhelmed by the effect of the electric field.<sup>52</sup> Mobilities and diffusivities of the individual species may be ascertained, at least in the dilute solution limit where ion–ion interactions are minimal.<sup>43</sup> The present measurements fall into this category. By extrapolating electrolyte conductivity measurements in human nail plate to infinite dilution and analyzing the results in conjunction with independently measured cation transport numbers, we were able to discover the pattern of behavior shown in Figure 3. There are clear differences between cations and anions in the effective diffusivities in nail inferred from these measurements. Both show a strong size dependence, describable over the range  $1 \text{ \AA} < r_{SE} < 5 \text{ \AA}$  in terms of a power law with an exponent of  $-1.75 \pm 0.27$ , but the magnitudes of the fitted curves vary between charge types, with those for cations exceeding those for comparably sized anions by about a factor of 3. These results differ from a comparable analysis of ionic transport in skin, where the corresponding power law exponent was found to be  $-0.65 \pm 0.29$  and there was no discernable difference in the magnitude of diffusivity for cations and anions.<sup>25,26</sup> A graphical comparison of these results is shown in Figure 4. It is evident that nail is considerably more size selective than skin for transverse transport of small ions.

**Table 4**  
Aqueous Diffusivities at Infinite Dilution Corrected to 32°C and 2 Measures of Ionic Size

Ionic Species	MW (Da)	$D_{soln}^0 \times 10^7$ (cm <sup>2</sup> /s)		$r_{SE}^a$ (Å)	$r_H^b$ (Å)
		Observed <sup>c</sup>	Literature <sup>d</sup>		
Na <sup>+</sup>	23	161.8	159.1	1.84	3.58
K <sup>+</sup>	39	239.0	233.4	1.25	3.31
TEA <sup>+</sup>	130	97.6	103.5	2.82	4.00
Ca <sup>2+</sup>	40	81.6	94.5	3.09	4.12
OlamH <sup>+</sup>	61	138.5	134.0	2.18	3.70
TPP <sup>+</sup>	339	57.1	—	5.11 <sup>f</sup>	5.16
MTPP <sup>+</sup>	277	61.9	—	4.72 <sup>f</sup>	4.94
Cl <sup>-</sup>	35	252.7	242.4	1.21	3.32
Br <sup>-</sup>	80	257.0	248.1	1.18	3.30
SO <sub>4</sub> <sup>2-</sup>	96	122.0	127.0	2.30	3.79
Bz <sup>-</sup>	121	104.4	102.5	2.85	4.03
Ac <sup>-</sup>	59	127.3	129.9	2.25	3.75

MW, molecular weight.

<sup>a</sup> Stokes–Einstein radius calculated from Equation 9 and literature value of  $D_{soln}^0$ .

<sup>b</sup> Hydrated ionic radius.<sup>44</sup>

<sup>c</sup> Calculated from data in column 3 of Table 3.

<sup>d</sup> Calculated from data in column 4 of Table 3.

To place the size dependencies in a familiar context, we fit a cylindrical pore-hindered diffusion model for uncharged solutes (centerline approximation) to both the skin and nail data in Figure 4. Details are given in the Supplementary Material to this report. The results are shown as dotted red lines in Figure 4. The optimum pore radius for the skin data (Fig. 4a) was 16 Å (range 12–28 Å), whereas the nail data (Fig. 4b) yielded a minimum centered at 11 Å (range 9–14 Å). The pore model with a small pore radius predicted a substantial convex curvature to log–log plots of diffusivity versus size, which is not evident in Figure 4b. For the nail, we considered also the fiber matrix models for uncharged solutes described in Baswan et al.<sup>27</sup> (see Supplementary Material). As in that report, neither of the models considered accurately described the results. The size selectivity of the fiber matrix models was closer to that of nail plate than the cylindrical pore model; however, the absolute values of the calculated hindrance factors were substantially in error. Although nail plate seems (to us) to be a dense fiber matrix comprised predominately of keratin, it is evident that more development of diffusion theory for such systems is required to explain its permeability.

The analysis in this report, summarized in Equations 7–9 and described in more detail elsewhere,<sup>25</sup> is the standard analysis for solution electrochemistry. It is based on limiting ionic conductance determined from Kohlrausch plots, in which conductivity is plotted

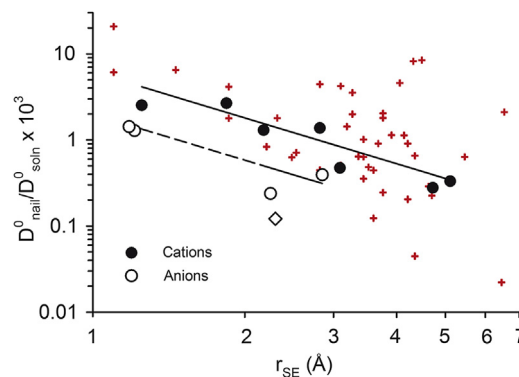


**Figure 3.** Double logarithmic plot of the effective diffusivity of ions in the nail plate relative to their diffusivity in solution plotted versus Stokes–Einstein radius,  $r_{SE}$ . The solid lines correspond to Equation 10 in the text. Sulfate ion (open diamond) was excluded from the regression analysis. The red crosses represent passive diffusion data for uncharged solutes in nail assembled by Baswan et al.<sup>27</sup>

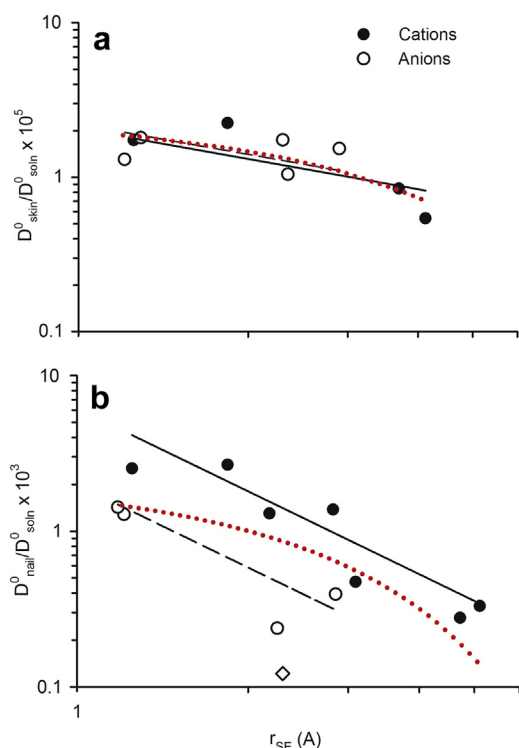


**Figure 4.** Effective ionic diffusivity ratios with respect to aqueous solution for (a) skin<sup>25,26</sup> and (b) nail (this study), plotted as a function of hydrodynamic radius of the ion. The straight lines correspond to the power law regressions described in LaCount and Kasting<sup>26</sup> and Equation 10, respectively (solid lines, cations; dashed lines, anions). The dotted red lines correspond to fits of a cylindrical pore model to the data, as described in the Supplementary Material. (a)  $r_p = 16 \text{ \AA}$ ,  $\epsilon/\tau = 2.6 \times 10^{-5}$ ; (b)  $r_p = 11 \text{ \AA}$ ,  $\epsilon/\tau = 1.88 \times 10^{-3}$ .

versus the square root of the molar electrolyte concentration,  $c$ . For solutions,  $c$  is known precisely, but for tissues bathed in an external electrolyte only the external concentration is known. Consequently the values of  $\Lambda_{\text{nail}}^0$  determined in this study reflect a tissue-solution partition coefficient that is not present in solution measurements. This is why cations and anions of comparable size may have different values of effective diffusivity in the nail plate,  $D_{\text{nail}}^0$ . Due to the negative charge associated with nail keratin, cations partition more favorably into the membrane than do anions, resulting in higher internal concentrations,  $c_{\text{nail}}$ , and higher limiting ionic conductivities,  $\lambda_{\text{nail}}$ .

The question may be asked as to whether the results of this analysis may be used to predict iontophoretic transport in nail of other ions or the passive diffusion results of Kobayashi et al.<sup>48</sup> For

larger ions, it is possible to estimate radii from correlations with molecular weight developed for uncharged solutes as discussed by Ibrahim et al.<sup>53</sup> Solution diffusivities can then be calculated by rearranging Equation 9 and effective diffusivity in nail can be estimated by extrapolation of Equation 10. However, under passive diffusion conditions *in vivo*, ionic drug transport is coupled to other ions in the donor solution and to those in the viable skin layers, especially sodium and chloride.<sup>52</sup> Quantitative analysis of this problem for charged membranes and polyvalent ions involves solution of a complicated boundary value problem that will not be discussed here.<sup>54</sup> An update on this solution may be found in a recent PhD thesis from our group<sup>55</sup>; however, neither the original analysis nor the update deal with the hindrance provided by the keratin fiber matrix in the nail plate. Nevertheless, we show in Figure 3 that the present estimates of the ratio  $D_{\text{nail}}^0/D_{\text{soln}}^0$  are comparable with a similar ratio calculated for uncharged solutes in nail by Baswan et al.<sup>27</sup> The conductivity data are more precise than the passive diffusion data and allow a better estimate of the size dependence of diffusion for solutes in the 1–5 Å range. A modest extrapolation of the regressions given in Equation 10 and Figure 3, combined with appropriate electrostatic coupling,<sup>52</sup> can be anticipated to yield plausible diffusion constants in human nail plate for therapeutic antifungal drugs having radii of 5–7 Å.<sup>27</sup>

So how, indeed, can this information be synthesized to predict iontophoretic drug delivery through nail? We present in Table 5 a stepwise procedure that may be anticipated to yield useful estimates. Assumptions implicit in this analysis include (1) the electroneutrality approximation for solution of the Nernst–Planck flux equations<sup>56</sup> is valid for the nail system; (2) electro-osmotic effects are minimal (see Hao and Li<sup>57</sup> for a discussion); and (3) ion transport numbers remain constant at the target current densities. Steps 2 and 3 require experience with electrolyte transport in membranes; nevertheless, the process is well defined. The biggest uncertainties are the estimation of membrane charge effects in step 2 and the possible influence of electro-osmosis. A test of the proposed procedure is warranted.

## Conclusions

Limiting ionic mobilities and diffusivities of 12 ionic species in solution and hydrated nail plate were determined by performing *in vitro* conductivity and EMF experiments with 17 electrolytes. Permeability of the nail plate for cationic transport was found to be related to the size and valence of the cation; it was a 1.3- to 1.5-fold increment in transport number relative to solution values for the small, monovalent cations  $\text{Na}^+$  and  $\text{K}^+$  but vanished for large or polyvalent ions in the presence of smaller counterions. An inverse relationship between effective ionic diffusivity in nail and size, describable in terms of a power law with an exponent of  $-1.75$ , was

**Table 5**

Procedure for Estimating Iontophoretic Delivery in Nail From Effective Ionic Diffusivity Data and Regression (Eq. 10)

1. Assemble molar concentrations and valence of each diffusible ion present in the drug delivery compartment and in the body. For the latter, an electrolyte composition of 0.154 M NaCl, pH 7.4, is a suitable starting point.
2. Estimate hydrodynamic radii,  $r_{\text{SE}}$ , for all ions and then calculate their aqueous diffusivities at skin temperature using the Stokes–Einstein relationship (Eq. 9). Estimate effective diffusivities in nail using Equation 10. If the pH in the donor compartment is substantially lower than the range 5.5–7.8 represented by Equation 10, use a judicious estimate of the fixed charge on the nail plate to appropriately adjust cation and anion diffusivities within the range bounded by Equation 10. For example, if the pH of the donor compartment was 4, the fixed charge of the nail plate would approach zero, and cation and anion diffusivities for similar sized species would be expected to be equal.
3. (a) Compositions containing monovalent ions only: Use the Nernst–Planck solution for uncharged membranes under the electroneutrality approximation<sup>56</sup> to estimate the flux of each ion as a function of potential drop across the membrane,  $\Delta\phi$ . Cases 1 and 2 in the cited reference give examples of how to do this. Calculate ion transference numbers,  $t_i$ , for each diffusing species by dividing ion flux,  $J_i$ , by the total calculated iontophoretic current,  $I_{\text{calc}}$ , associated with  $\Delta\phi$ . (b) Compositions containing monovalent and polyvalent ions: The Nernst–Planck solution for ions of multiple valences in charged membranes<sup>54,55</sup> must be used in lieu of Kasting and Keister<sup>56</sup> to calculate  $J_i$  and  $t_i$ . Spreadsheets implementing these calculations are available from the authors.
4. Calculate the flux of the ion of interest as a function of the experimental iontophoretic current,  $I_{\text{exp}}$ , as  $J_i = t_i \times I_{\text{exp}}$ .

found for both cations and anions. Under the assumption that the size effect was the same for both species, effective diffusivities of cations in nail were more than 3-fold greater than anions of comparable size, very likely reflecting the preferential partitioning of cations into the negatively charged nail plate. A method for using this information to predict transungual iontophoretic delivery in nail is proposed.

## Acknowledgements

This work was supported by a grant from the NIH (GM063559). The opinions expressed in this paper are those of authors and not endorsed by the NIH. The authors thank Jinsong Hao and Johannes Nitsche for helpful discussions.

## References

- Elewski BE, Charif MA. Prevalence of onychomycosis in patients attending a dermatology clinic in northeastern Ohio for other conditions. *Arch Dermatol*. 1997;133(9):1172–1173.
- Gupta AK, Jain HC, Lynde CW, Watteel GN, Summerbell RC. Prevalence and epidemiology of unsuspected onychomycosis in patients visiting dermatologists' offices in Ontario, Canada—a multicenter survey of 2001 patients. *Int J Dermatol*. 1997;36(10):783–787.
- Ghannoum MA, Hajjeh RA, Scher R, et al. A large-scale North American study of fungal isolates from nails: the frequency of onychomycosis, fungal distribution, and antifungal susceptibility patterns. *J Am Acad Dermatol*. 2000;43(4):641–648.
- Pierard G. Onychomycosis and other superficial fungal infections of the foot in the elderly: a pan-European survey. *Dermatology*. 2001;202(3):220–224.
- Botek G. Fungal nail infection: assessing the new treatment options. *Cleve Clin J Med*. 2003;70(2):110–114, 117–118.
- Kaur R, Kashyap B, Bhalla P. Onychomycosis—epidemiology, diagnosis and management. *Ind J Med Microbiol*. 2008;26(2):108–116.
- Vejnovic I, Huonder C, Betz G. Permeation studies of novel terbinafine formulations containing hydrophobins through human nails in vitro. *Int J Pharm*. 2010;397(1–2):67–76.
- Hao J, Smith KA, Li SK. Chemical method to enhance transungual transport and iontophoresis efficiency. *Int J Pharm*. 2008;357(1–2):61–69.
- Nair AB, Sammeta SM, Kim HD, Chakraborty B, Friden PM, Murthy SN. Alteration of the diffusional barrier property of the nail leads to greater terbinafine drug loading and permeation. *Int J Pharm*. 2009;375(1–2):22–27.
- Brown MB, Khengar RH, Turner RB, et al. Overcoming the nail barrier: a systematic investigation of unguinal chemical penetration enhancement. *Int J Pharm*. 2009;370(1–2):61–67.
- Salter SA, Ciocon DH, Gowrishankar TR, Kimball AB. Controlled nail trephination for subungual hematoma. *Am J Emerg Med*. 2006;24(7):875–877.
- Maeda N, Mizuno N, Ichikawa K. Nail abrasion: a new treatment for ingrown toe-nails. *J Dermatol*. 1990;17(12):746–749.
- Behl PN. Abrasion in the treatment of nail disorders. *Ind J Dermatol*. 1973;18(4):77–79.
- Jeremiase HP. Treatment of nail infections with griseofulvin combined with abrasion. *Trans St Johns Hosp Dermatol Soc*. 1960;45:92–93.
- Repka MA, Mididoddi PK, Stodghill SP. Influence of human nail etching for the assessment of topical onychomycosis therapies. *Int J Pharm*. 2004;282(1–2):95–106.
- Amichai B, Mosckovitz R, Trau H, et al. Iontophoretic terbinafine HCL 1.0% delivery across porcine and human nails. *Mycopathologia*. 2010;169(5):343–349.
- Amichai B, Nitzan B, Mosckovitz R, Shemer A. Iontophoretic delivery of terbinafine in onychomycosis: a preliminary study. *Br J Dermatol*. 2010;162(1):46–50.
- Delgado-Charro MB. Iontophoretic drug delivery across the nail. *Exp Opin Drug Deliv*. 2012;9(1):91–103.
- Dutet J, Delgado-Charro MB. Electroosmotic transport of mannitol across human nail during constant current iontophoresis. *J Pharm Pharmacol*. 2010;62(6):721–729.
- Manda P, Sammeta SM, Repka MA, Murthy SN. Iontophoresis across the proximal nail fold to target drugs to the nail matrix. *J Pharm Sci*. 2012;101(7):2392–2397.
- Murthy SN, Waddell DC, Shivakumar HN, Balaji A, Bowers CP. Iontophoretic permselective property of human nail. *J Dermatol Sci*. 2007;46(2):150–152.
- Nair AB, Kim HD, Chakraborty B, et al. Ungual and trans-ungual iontophoretic delivery of terbinafine for the treatment of onychomycosis. *J Pharm Sci*. 2009;98(11):4130–4140.
- Nair AB, Vaka SR, Sammeta SM, et al. Trans-ungual iontophoretic delivery of terbinafine. *J Pharm Sci*. 2009;98(5):1788–1796.
- Narasimha Murthy S, Wiskirchen DE, Bowers CP. Iontophoretic drug delivery across human nail. *J Pharm Sci*. 2007;96(2):305–311.
- LaCount TD, Kasting GB. Human skin is permselective for the small, monovalent cations sodium and potassium but not for nickel and chromium. *J Pharm Sci*. 2013;102(7):2241–2253.
- LaCount TD, Kasting GB. Erratum: Human skin is permselective for the small, monovalent cations sodium and potassium but not for nickel and chromium. *J Pharm Sci*. 2015. online in advance of print.
- Baswan S, Li SK, Kasting GB. Diffusion of uncharged solutes through human nail plate. *Pharm Dev Technol*. 2014;1–6. <http://dx.doi.org/10.3109/10837450.2014.991876> [Epub ahead of print].
- Gunt HB, Miller MA, Kasting GB. Water diffusivity in human nail plate. *J Pharm Sci*. 2007;96(12):3352–3362.
- Leider M, Buncke CM. Physical dimensions of the skin: determination of the specific gravity of skin, hair, and nail. *Arch Dermatol*. 1954;69(5):563–569.
- Ramos PM. A four-terminal water-quality-monitoring conductivity sensor. *IEEE Trans Instrum Meas*. 2008;57(3):577–583.
- Plonsey R, Barr R. The four-electrode resistivity technique as applied to cardiac muscle. *IEEE Trans Biomed Eng BME*. 1982;29(7):541–546.
- Keston AS. A silver-silver bromide electrode suitable for measurements in very dilute solutions. *J Am Chem Soc*. 1935;57(9):1671–1673.
- Smith KA, Hao J, Li SK. Influence of pH on transungual passive and iontophoretic transport. *J Pharm Sci*. 2010;99(4):1955–1967.
- Tezel A, Sens A, Tuchscherer J, Mitragotri S. Synergistic effect of low-frequency ultrasound and surfactants on skin permeability. *J Pharm Sci*. 2002;91(1):91–100.
- Robinson R, Stokes R. *Electrolyte Solutions*. 2<sup>nd</sup> (rev) ed. London: Butterworths; 1970:284–288.
- Ersoz M. Transport numbers in biomembranes from EMF measurements. *Bio-phys Chem*. 2001;94(3):237–243.
- Compañ V, Sørensen TS, Andrio A, López L, de Abajo J. Transport numbers from initial time and stationary state measurements of EMF in non-ionic polysulphonic membranes. *J Memb Sci*. 1997;123(2):293–302.
- Aguilella V, Kontturi K, Murtoimäki L, Ramirez P. Estimation of the pore size and charge density in human cadaver skin. *J Control Release*. 1994;32(3):249–257.
- Ottøy M, Førland T, Ratkje SK, Møller-Holst S. Membrane transference numbers from a new EMF method. *J Memb Sci*. 1992;74(1–2):1–8.
- Jonsson G, Benavente J. Determination of some transport coefficients for the skin and porous layer of a composite membrane. *J Memb Sci*. 1992;69(1–2):29–42.
- Kaimakov EA, Varshavskaya NL. Measurement of transport number in aqueous solutions of electrolytes. *Russian Chem Rev*. 1966;35(2):89.
- Sinko PA. *Martin's Physical Pharmacy and Pharmaceutical Sciences*. 6<sup>th</sup> ed. Philadelphia, PA: Lippincott Williams & Wilkins; 2011.
- Bockris JOM, Reddy AKN. *Modern Electrochemistry*. New York, NY: Plenum Press; 1970.
- Nightingale ER. Phenomenological theory of ion solvation. Effective radii of hydrated ions. *J Phys Chem*. 1959;63:1381–1387.
- Gierer A, Wirtz K. Molekulare theorie der mikroreibung. *Z Naturforsch*. 1953;8a:532–538.
- Baden H. The physical properties of nail. *J Invest Dermatol*. 1970;55:115–137.
- Curran PF, Schultz SG. *Transport Across Membranes: General Principles. Handbook of Physiology*. Baltimore, MD: Waverly Press; 1968:1217–1243.
- Kobayashi Y, Komatsu T, Sumi M, et al. In vitro permeation of several drugs through the human nail plate: relationship between physicochemical properties and nail permeability of drugs. *Eur J Pharm Sci*. 2004;21(4):471–477.
- Mertin D, Lippold BC. In-vitro permeability of the human nail and of a keratin membrane from bovine hooves: prediction of the penetration rate of antimicrobics through the nail plate and their efficacy. *J Pharm Pharmacol*. 1997;49(9):866–872.
- Kobayashi Y, Miyamoto M, Sugibayashi K, Morimoto Y. Drug permeation through the three layers of the human nail plate. *J Pharm Pharmacol*. 1999;51:271–279.
- Walters KA, Flynn GL, Marvel JR. Physicochemical characterization of the human nail: solvent effects on the permeation of homologous alcohols. *J Pharm Pharmacol*. 1985;37(11):771–775.
- Cussler EL. *Diffusion: Mass Transfer in Fluid Systems*. 3<sup>rd</sup> ed. Cambridge, UK: Cambridge University Press; 2009:580.
- Ibrahim R, Nitsche JM, Kasting GB. Dermal clearance model for epidermal bioavailability calculations. *J Pharm Sci*. 2012;101(6):2094–2108.
- Schlögl R. Electrodiffusion in free solution and charged membranes. *Z Phys Chem*. 1954;1:305–339.
- LaCount TD. *Skin absorption modeling of metal allergens via the polar pathway*. PhD thesis. Cincinnati, OH: University of Cincinnati; 2014.
- Kasting GB, Keister JC. Application of electrodiffusion theory for a homogeneous membrane to iontophoretic transport through skin. *J Control Release*. 1989;8:195–210.
- Hao J, Li SK. Mechanistic study of electroosmotic transport across hydrated nail plates: effects of pH and ionic strength. *J Pharm Sci*. 2008;97(12):5186–5197.